At-line validation of Optical Coherence Tomography as in-line/at-line Coating Thickness Measurement Method

Matthias Wolfgang[1], Anna Peter[1], Patrick Wahl[1],
Daniel Markl[2,3], J. Axel Zeitler[4], Johannes G. Khinast[1,5,*]

[1]Research Center Pharmaceutical Engineering GmbH, Graz, Austria
[2]Institute of Pharmacy and Biomedical Sciences, University of Strathclyde, Glasgow, UK
[3]EPSRC Centre for Innovative Manufacturing in Continuous Manufacturing and Crystallisation, University of Strathclyde, Glasgow, UK
[4]Department of Chemical Engineering and Biotechnology, University of Cambridge, Cambridge, UK
[5]Institute for Process and Particle Engineering, Graz University of Technology, Graz, Austria

*corresponding authors electronic address: khinast@tugraz.at

ABSTRACT

Optical Coherence Tomography (OCT) is a promising technology for monitoring of pharmaceutical coating processes. However, the pharmaceutical development and manufacturing require a periodic validation of the sensor's accuracy. For this purpose, we propose polyethylene terephthalate (PET) films as a model system, which can be periodically measured during manufacturing coating monitoring via OCT. This study proposes a new approach addressing the method validation requirement in the pharmaceutical industry and presents results for complementary methods. The methods investigated include direct measurement of the layer thickness using a micrometer gauge as reference, X-ray micro computed tomography, transmission and reflectance terahertz pulsed imaging, as well as 1D- and 3D-OCT. To quantify the significance of OCT for pharmaceutical coatings, we compared the OCT results for commercial Thrombo-ASS and Pantoloc tablets with direct measurements of coating thickness via light microscopy of microtome cuts. The results of both methods correlate very well, indicating high intra- and inter-tablet variations in the coating thickness for the commercial tablets. The light microscopy average measured coating thickness of Thrombo-ASS (Pantoloc) was 71.0 µm (83.7 µm), with an inter-coating variability of 8.7 µm (6.5 µm) and an intra-coating variability of 2.3 µm to 9.4 µm (2.1 µm to 6.7 µm).

Keywords (4-6): optical coherence tomography (OCT); terahertz pulsed imaging (TPI); micro computed tomography (µCT); reference material; coating thickness variability

1. INTRODUCTION

In the last 28 years optical coherence tomography (OCT) has become an established standard technology in medicine and the clinical practice (de Boer et al., 2017). Apart from medical applications, OCT can provide valuable insights into various structured materials when non-destructive testing is required (Nemeth et al., 2013). In 2009, Mauritz et al. demonstrated first attempts to investigate pharmaceutical coatings by means of OCT(Mauritz et al., 2010), opening a new field of applications for this technology. In the years after, several research groups, including our own, have demonstrated that OCT is a very promising technology for non-destructive monitoring of pharmaceutical film coating

processes (Lin et al., 2018) for tablets (Koller et al., 2011; Lin et al., 2015; Markl et al., 2015a, 2014) and pellets (Li et al., 2014; Markl et al., 2015b). The literature indicates that OCT can provide information about critical material attributes, such as coating thickness, inner structure and homogeneity (intra- and inter-coating variability) of pharmaceutical coatings applied to tablets (Dong et al., 2017; Lin et al., 2017; Markl et al., 2018) and pellets (Li et al., 2014; Wolfgang et al., 2019). As a direct measurement technique, OCT does not require the development and maintenance of chemometric models for data interpretation, as is typically the case for near-infrared (Möltgen et al., 2013; Wahl et al., 2019) or Raman spectroscopy (Barimani and Kleinebudde, 2017; Müller et al., 2010). In contrast to more established spectroscopic approaches, OCT can reference the measured signals to known spectral distances and natural constants (speed of light). The only material-dependent variable is the refractive index of the materials tested. With a high axial resolution of a few microns and a scanning speed of up to 250 kHz, OCT makes it possible to characterize coating structures within microseconds.

Besides medical and pharmaceutical applications, low coherence interferometry (upon which OCT is based) can be used to measure coating thickness (Kühnhold et al., 2015; Manallah et al., 2015) and optical properties of polymer films, such as topography (Ghim et al., 2013), roughness (Yoshino et al., 2017) and refractive indices (Yen et al., 2014). Also inline monitoring of coating process applications in industrial coaters (both for tablets and pellets) have been demonstrated (Sacher et al., 2019). Nevertheless, before introducing industrial OCT systems into the pharmaceutical industry, it is critical to demonstrate that the measurements are reproducible and accurate. This is required by Good Manufacturing Practice (GMP) requirements. Surprisingly, to the best of the authors' knowledge, there is no commonly available or conventional standard reference material that can be readily used to validate industrial OCT systems in terms of coating thickness measurements suitable for pharma applications. There has been work published discussing the need for OCT depth calibration in the past. Approaches range from precision laser-etched nanoparticles in polyurethane-resin (Gabriele Sandrian et al., 2012), to photolithographic 3D printing, mimicking the commonly known USAF 1951 test chart (Hu et al., 2014) in a tree-dimensional way. Even highly sophisticated 3D printed eye phantoms simulating human eyes with retinal features have been presented (Corcoran et al., 2015), but none of them fulfils the requirements for an industrial OCT reference target.

Thus, the goal of this study was to identify reference materials suitable for pharmaceutical OCT validation and to propose a possible solution by periodically validating the in-process OCT via measurements of standardized films. Since Terahertz pulsed imaging (TPI) and OCT have been reported to be complementary technologies with respect to pharmaceutical coating investigation (Zhong et al., 2011), it would be additionally beneficial if the reference material would also be suitable for TPI. There has been work presented for TPI where polymer foils aided as a reference (Zeitler et al., 2007). In addition to identifying a suitable reference material, measurements of commercial tablets acquired using a commercial pharma OCT system were validated to demonstrate that the OCT readings are accurate and valid, as well as to illustrate the degree of coating thickness variation in the tablets.

2. MATERIALS AND METHODS

2.2 Material Selection Considerations

Currently, only one dedicated commercial OCT reference target is available. It is made of laser-structured fused silica and manufactured and distributed by Arden Photonics. The Arden Photonics

reference target APL-OP01 (Arden Photonics Ltd., Solihull, United Kingdom) is intended to be a reference and validation target for ultra-high resolution OCT (UHR-OCT) used in ophthalmic surgery. It provides a reference for the point spread function, sensitivity, lateral resolution and distortion (Arden Photonics Ltd, 2018), but not for the layer thickness that could be used for determining the coating layer thicknesses. Unfortunately, the existing reference target is not suitable for validation of industrial OCT equipment since its structures have a lateral linewidth of less than 2 µm (manufacturer's specification). As such, the lines are too thin to be applied in an industrial OCT sensor whose lateral resolution is typically within the range of 8-20 µm (in air). Additionally, several specific requirements have to be taken into account when applying equipment in pharmaceutical manufacturing environments, including the Good Manufacturing Practice (GMP) guidelines, hygiene design guidelines, availability of material certificates (for FDA approval), resistance of used materials against organic solvents, detergents, moisture, mechanical stress (e.g., glass breakage) and heat. Furthermore, a suitable reference material for industrial validation of OCT equipment ideally has to have additional optical properties, e.g., a refractive index similar to that of the materials tested, uniform optical properties and a traceable quality.

After investigating several potential materials, such as the anodization layer of anodized aluminium (not accurate enough in terms of reproducible thickness), several glasses (contamination of pharmaceutical processes with glass fragments is a major issue that may have legal consequences) and plastics, we found bi-axially oriented polyethylene terephthalate (PET) foils to be the most promising one. The specific reasons for selecting it are its well-known physical properties and a refractive index similar to that of dried pharmaceutical coatings. Moreover, no other materials with a suitable refractive index, such as polypropylene (PP), polyamides (PA) and polyethylene-naphthalate (PEN), were available within the desired range of thickness (3-300 µm).

2.3 Biaxially Oriented Polyethylene Terephthalate Films (PET)

PET appears to be a reference material suitable for OCT standards. The production process for PET films has been carefully optimized to deliver highly reproducible products since one of its main applications is the manufacturing of dielectric separation layers for capacitors. With that regard, a reproducible and homogeneous film thickness is crucial since it directly affects the dielectric strength and achievable specific capacitance. In addition, the constant and highly reproducible optical properties of PET films, no water absorption, low thermal expansion coefficient and resistance to all chemicals typically used in the pharmaceutical industry suggest that this material can be applied as an OCT reference standard. Considering the effects of ageing, PET is a persistent material. What is a drawback from an ecological point of view is an advantage for the expected shelf-life of PET foils as a reference material. Studies to the accelerated degradation of PET (Bell, 2016) and the material properties provided by the manufacturers indicate that under normal conditions the degradation is neglectable, considering the material is stored at room temperature and constant humidity without exposing it to UV radiation. Based on our investigations we would expect no altering of critical properties for our intended use within years. In terms of mechanical stability the material is quite resistant, nevertheless we put all foil samples in a sample holder to ensure that they are straight and protected against damage. However, PET has one drawback: during the manufacturing process the films become bi-axially stretched and birefringent (Amborski and Flierl, 1953). To account for this, the PET-foils of a validation or calibration target should always be measured in the same orientation relative to the OCT sensor. This was guaranteed by the use of the above mentioned foil holder. Moreover, the birefringent behaviour is not a major problem for the intended use, because the

refractive indices in plane of PET foils are nearly the same (less than 0.002 deviation) and only the index orthogonal to the foil plane deviates, guaranteeing reproducible measurements when using a defined geometry during reference measurements along the plane.

The suitability of PET foils as a reference standard was examined based on experiments using the brand product “Mylar A” manufactured by DuPont (Dupont Teijin Films, Dumfries, United Kingdom) with nominal sheet thicknesses of 19, 36, 50, 75, 100, 125 and 190 µm. According to the manufacturer, the films have a thickness tolerance of +/- 5% (based on weight). Characterization of the foils as a validation target was carried out using several measurement technologies described below. The physical properties of Mylar foils were previously summarized by DuPont (DuPont Teijin Films, 2003) and in addition to the Mylar A foils, we investigated Hostaphan RN foils manufactured by Mitsubishi (Mitsubishi Polyester Film GmbH, Wiesbaden, Germany). Since both materials are produced in the same manner and reportedly have the same electrical and physical properties, they should have the same behaviour when tested. For this additional set of samples the measurements were performed only via OCT over an extended thicknesses range of 12-350 µm (12, 23, 50, 75, 100, 190 and 350 µm) in order to establish if the materials are interchangeable as an OCT reference material. Based on the combined measurements for both PET materials, we examined the linearity of results within the desired thickness range.

It has been reported that biaxially stretched PET foils are prone to slight deviations in the refractive index along the thickness-axis with an increasing thickness (Elman et al., 1998) as a result of the manufacturing process. To that end, we tested both materials for their linearity throughout the entire thickness range to determine if this is an issue for industrial OCT systems.

2.4 Micrometer Gauge Measurements

As a reference method, we carried out direct measurements of the foil sheets using a precision micrometer gauge (Mitutoyo QuantumMike, MDE-25MJ, 0-25 mm) with a resolution of 1 µm, (Mitutoyo Europe, Neuss, Germany). The micrometer gauge utilises a torque-regulation mechanism to maintain the contact pressure constant between the measurements. In order to study the homogeneity of film thickness, between 111 and 134 measurements were taken in various positions for each foil.

2.5 X-Ray Micro Computed Tomography

X-ray micro computed tomography (XµCT) measurements of films were performed using a Bruker Skyscan 1172 (Bruker microCT, Kontich, Belgium). For this purpose, the films were stacked between separating layers of ordinary copier paper sheets (80 g/m²) and the entire stack was measured in a single acquisition. The images were recorded with a voxel size of 1.49 µm and the layer thickness was calculated based on the XµCT images in ten positions for each foil.

2.6 Terahertz Pulsed Imaging

Terahertz time-domain measurements were performed using a TeraPulse 4000 (TeraView Ltd., Cambridge, United Kingdom). Transmission and reflection measurements were undertaken to infer the refractive index and measure the foil thicknesses. Transmission measurements were acquired under nitrogen gas purge. The reflectance measurements were accomplished using a fiber-coupled probe head with a fixed angle of reflection of 30°. In all Terahertz measurements, the foils were

inclined at 7° relative to the terahertz beam in order to prevent multiple internal reflections that would result in Fabry-Pérot resonance artefacts during the acquisition.

The refractive index for the Terahertz measurements was extracted from the transmission measurements of foils with thickness of 100, 125 and 190 µm using the micrometer gauge measurements as the reference method and was calculated to be 1.765 +/- 0.011. Based on this refractive index, we estimated an axial resolution limit of ≈ 35 µm for measuring the thickness of films via the Terahertz reflection method by directly resolving the time-of-flight peaks from two subsequent reflections in the time-domain waveform. Since in the terahertz measurements only a single point on each sample was measured, no standard deviations in the spatial thickness variation of each sample were recorded.

2.7 Optical Coherence Tomography

OCT measurements were performed using two different OCT systems. To acquire full volume information, an in-house 3D OCT prototype as described in (Markl et al., 2018) was used. Fully automated 1D OCT measurements were carried out via a commercial pharma OCT system (OSeeT Pharma 1D, Phyllon, Austria) equipped with exchangeable perforated rotating drums with an outer diameter of 200 mm. In this setup it is possible to move samples (e.g., foils) mounted along the circumference of the drum in front of a static 1D-OCT sensor in a reproducible manner at a pre-defined speed or, alternatively, to mimic the behaviour of a moving tablet bed when the tablets are placed inside the drum, with the sensor scanning the interior of the moving tablet bed through the perforation. All measurements in the drum-setup were performed using the drum rotating at 35 rpm to prevent artefacts due to various circumferential velocities.

Both OCT systems have a super luminescent diode as light-source with a central wavelength of 832 nm and a spectral bandwidth of 75 nm, resulting in a theoretical axial resolution of 4.1 µm (in air, n = 1). The chosen optical setup of the sensor head, as described in (Koller et al., 2011), results in a lateral resolution of 10 µm in the 3D configuration. The lateral resolution of the commercial 1D-OCT system is reported to be 14 µm based on the specifications of the system.

For all 3D-OCT measurements, the sensor exposure time was 30 µs and the idle time (for read-out and digitalization) was 1.9 µs, which resulted in an acquisition rate of 31.3 kHz. The latter corresponds to the number of single-depth scans (A-scans) per second, corresponding to a frame rate of 30.6 fps. All measurements for foils and tablets were performed en-face. In 1D measurements, the sensor exposure time was 4 µs and the idle time was 6 µs for read-out, digitization and evaluation, resulting in a real-time capable framerate of 97.66 fps. All samples measured by the 1D system were inclined at 5° to prevent multiple internal reflections that would otherwise result in Fabry-Pérot resonance artefacts during the acquisition.

The refractive index for the PET foils was determined prior to the OCT measurements based on an additional foil sample with a thickness of 50 µm, which was qualified according to ISO 534:2011-11 by an external facility (Technical Testing and Research Institute for Paper, Pulp and Fibre Technology, University of Technology, Graz, Austria). Based on the certified thickness and the pixel-distances in the OCT images, the refractive index for the light source (central wavelength and spectral distribution) was calculated based on 5 replicated volume measurements in various positions of the foil to be n = 1.615 $\pm$ 0.002 for Mylar and n = 1.707 $\pm$ 0.041 for Hostaphan, respectively. These refractive indices were

used for all PET evaluations of the respective materials and lead to theoretical axial resolutions of 2.5 µm for Mylar and 2.4 µm for Hostaphan.

The refractive indices for the tablet coatings measured were calculated based on OCT cross-sectional images of separate, additional tablet samples compared to microscopy images of the tablets in the position where the OCT image was acquired. The refractive indices were calculated to be $n = 1.48 \pm 0.02$ for the Thrombo ASS and $n = 1.45 \pm 0.02$ for the Pantoloc coating.

For the 3D OCT scans of PET-foils and for the tablets, the volumetric scans acquired were automatically evaluated by calculating the mean thickness and variation based on 524,288 individual A-scans for each sample. The scanned area of each sample was 3.12 mm x 3.12 mm in all measurements. Linearity measurements for the two PET materials were performed based on additional 3D volumetric scans.

2.8 Commercial Tablets Tested

50 commercially-available tablets of Thrombo-ASS (100 mg acetylsalicylic acid, G.L. Pharma GmbH, Lannach, Austria) and additional 50 tablets of Pantoloc (40 mg pantoprazole, Takeda Pharma GmbH, Vienna, Austria), all coated with a clear enteric coating, were purchased at a local pharmacy. All sample tablets were manually numbered on the tablet band using a fine liner (Staedler permanent Lumocolor, blue) that is transparent at the wavelengths applied by both OCT systems. All tablets were individually measured using the above-described 3D-OCT system, after which all tablets of one sample were measured at once via the 1D-OCT system in the rotating drum setup. For this purpose the whole sample was filled in the rotating drum, with the tablets moving free and randomly inside during acquisition, as is the case in an in-line scenario. Speed was chosen to ensure a good mixing to avoid acquisition of the same tablet parts during measurement. This was done to ensure the measurement of different tablets at different positions to gain a good statistical basis. The sensor in this setup was mounted outside the rotating drum scanning through the wholes inside the moving tablet bed.

Measurements via the in-house 3D OCT system were accomplished by recording cross-sectional images (B-scans) of all tablets and performing a subsequent graphical evaluation of the recorded images. For every B-Scan of the 3D measurements, the pixel distances between the top interface and the coating core-interface were manually determined using the graphical software ImageJ. Starting point for all evaluations was the centre of each B-scan with ten measurements in a distance of 100 µm on both sides covering a length of 2 mm in total. The coating thicknesses were calculated taking into account the corresponding refractive index. An automated evaluation of the 1D OCT measurements was performed using the software “OSeeT Pharma 1D v 3.2.3” provided with the 1D OCT system.

2.9 Microtome Cuts and Light Microscopy

Subsequent to the OCT measurements, 11 of the Thrombo ASS and 10 of the Pantoloc tablets were randomly chosen and examined off-line using light microscopy. The entire procedure was executed externally at the Center for Electron Microscopy (Graz, Austria). Following the 3D OCT measurements, all selected tablets were marked using a soft pencil (hardness 4B) to prevent damage to the tablet surface. The marking was performed so that the OCT measurement position could be reconstructed without affecting the position of the tablet surface where the OCT cross-sectional images were taken. The ultimate goal was to examine the coating structure as close to this position as possible. Next, the tablets were cut in half along the middle of the tablet band and both halves were embedded in epoxy resin Epofix (Struers GmbH, Willich, Germany) to fix and stabilize them for the microtome cuts. The

resin was used to prevent mechanical and thermal stress to the samples, which potentially could result in changes to the structures. The fixation time was 12 hours.

Once the resin had cured the embedded tablet halves were pre-cut close to the mark with a scalpel and dry microtomed into progressively thinner slices until a smooth surface finish for the interface in the location of the OCT measurements was achieved. Microtome cuts were performed with a precision microtome (Leica UC6, Leica Microsystems GmbH, Wetzlar, Germany) and examined microscopically using a Zeiss Axioplan with Axiocam IcC1 (Carl Zeiss Microscopy GmbH, Jena, Germany) at a magnification of 50x with direct illumination. The first microtome cuts were accomplished with a glass knife (slices starting at 5 and down to 1 µm thickness) to protect the histological diamond blade, which was used for the final thinnest slices (300 to 100 nm slices). Following this procedure allowed us to minimize any cross-contamination by smearing and plastic deformation of the coating material, preserving the coating structure as much as possible during microtoming. During microscopy, no deformation or smearing of coatings was detected. During light microscopy examination, a minimum of seven measurements per microtome cross section (tablets 2, 5, 12, 23, 32, 44) was performed. The remaining tablets were measured in 18 individual positions that refer to the tablet cap area.

3. RESULTS

3.2 Investigation of PET Foils

The experimentally determined film thickness measurements of the Mylar films for the various methods are summarized in Table 1. Common to all methods is a relatively small standard deviation of the measured film thickness, which is in most cases lower than the manufacturer's specified tolerance ~~and the micrometer gauge measurements~~. For the subsequent analysis, the micrometer gauge method was applied to represent the reference method for all foils tested. Results that deviated more than 10% from this reference value are highlighted by an asterisk. An illustration of all results is provided in Figures 1 and 2.

Table 1: Comparison of the film thickness measurements acquired using the various methods to determinate the film thickness of Mylar foils. Results with a deviation of over 10% from the micrometer gauge measurements, which acted as a reference throughout all measurement, are highlighted by an asterisk.

Foil [µm]	**Specification [µm]**	**Reference [µm]**	**Terahertz T [µm]**	**Terahertz R [µm]**	**XµCT [µm]**	**3D-OCT [µm]**	**1D-OCT [µm]**
19	19 ± 1.0	20.1 ± 2.1	23.5*	31.4*	20.5 ± 1.0	18.7 ± 0.8	18.3 ± 1.3
36	36 ± 1.8	36.7 ± 1.8	35.3	34.8	36.7 ± 1.1	35.2 ± 0.8	35.2 ± 1.1
50	50 ± 2.5	50.9 ± 1.4	51.0	44.2*	56.3 ± 3.2*	51.9 ± 0.4	53.5 ± 0.5
75	75 ± 3.8	74.0 ± 1.1	70.6	71.4	76.6 ± 2.7	77.6 ± 0.9	77.1 ± 1.9
100	100 ± 5.0	100.0 ± 1.0	98.0	96.8	99.0 ± 2.0	103.0 ± 0.5	101.2 ± 0.9
125	125 ± 6.3	124.6 ± 1.3	125.5	124.0	127.5 ± 1.8	126.8 ± 0.6	126.7 ± 0.9
190	190 ± 9.5	189.6 ± 1.9	192.1	188.6	187.5 ± 3.3	192.5 ± 0.5	189.1 ± 0.9
Comment	Specified by manufacturer	Uncertainty: 1.1 µm, k=2 (specification)	Transmission n = 1.765 ± 0.011	Reflection n = 1.765 ± 0.011	Voxel size: 1.49 µm	n = 1.615 ± 0.002	n = 1.615 ± 0.002

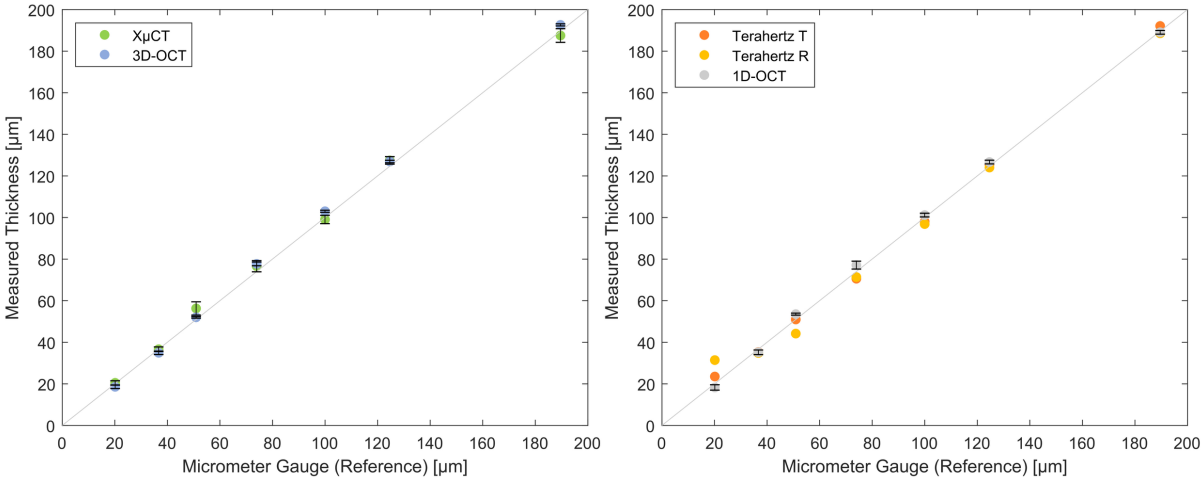

Figure 1: Comparison of average foil thicknesses with standard deviations in error bars evaluated in relation to micrometer gauge measurements as the reference. Since the terahertz measurements were performed as single-point measurements, no standard deviations are available for them. For the sake of clarity, the 3D and 1D methods are depicted on the left and right sides, respectively.

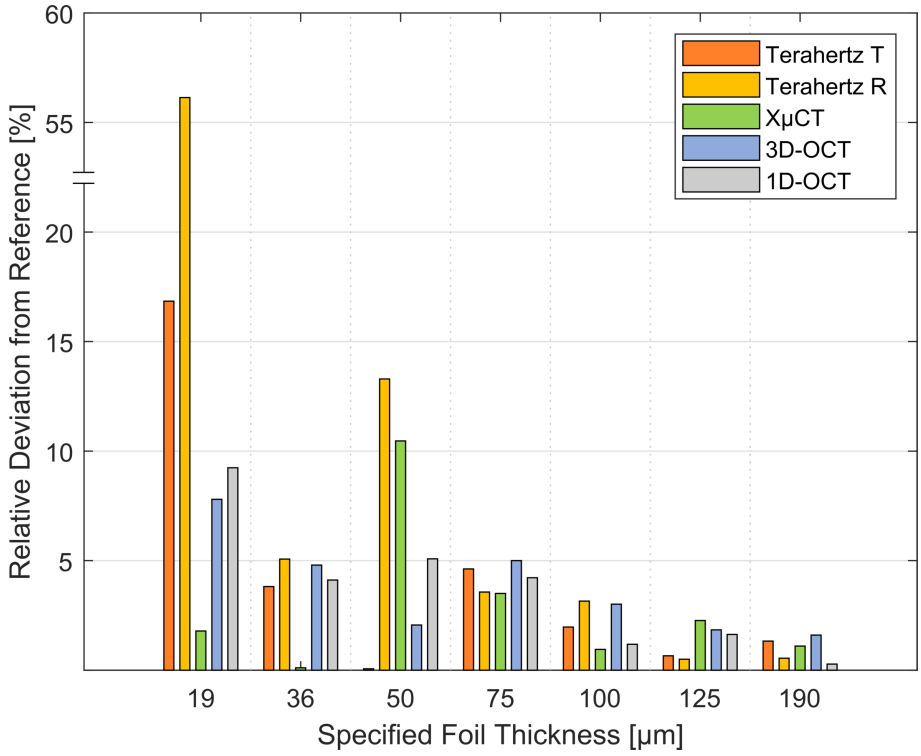

Figure 2: Comparison of relative deviations for each method in relation to the reference method (micrometer gauge measurements).

Sample preparation via stacked foils for the XµCT measurement facilitates the manual thickness evaluation of the acquired XµCT images. XµCT and OCT measurements resulted in 3D datasets, and both methods showed that the foils were highly uniform in terms of thickness. The XµCT measurements were evaluated by measuring the interface pixel distances using the software ImageJ at 10 different positions per foil. Based on the known voxel size of 1.49 µm, the corresponding film thickness was calculated. The XµCT results show the highest standard deviation among all techniques providing a standard deviation in the chosen setup.

Interestingly, only the OCT measurements have a consistently low standard deviation over the entire thickness range. The results for the OCT measurements indicated good linearity in the thickness range between 19 µm and 190 µm for Mylar and between 12 µm and 350 µm for the Hostaphan foils. Coefficients of determination and the root-mean-square error (RMSE) are summarized in Table 2.

Table 2: Linearity of methods compared to the micrometer gauge measurements as reference for the Mylar foils.

	Reference	Terahertz T	Terahertz R	XµCT	3D-OCT	1D-OCT
R^2	1.0000	0.9983	0.9864	0.9976	0.9992	0.9989
RMSE [µm]	0.000	2.270	5.283	2.631	2.501	1.999

A combination of all OCT results for both PET materials in relation to the reference method is provided in Figure 3. As expected, the linearity is good, even with different PET materials in the same fit and over a broad thickness range. The coefficient of determination for this mixed set was calculated to be $R^2 = 0.9993$ and RMSE = 2.15 µm.

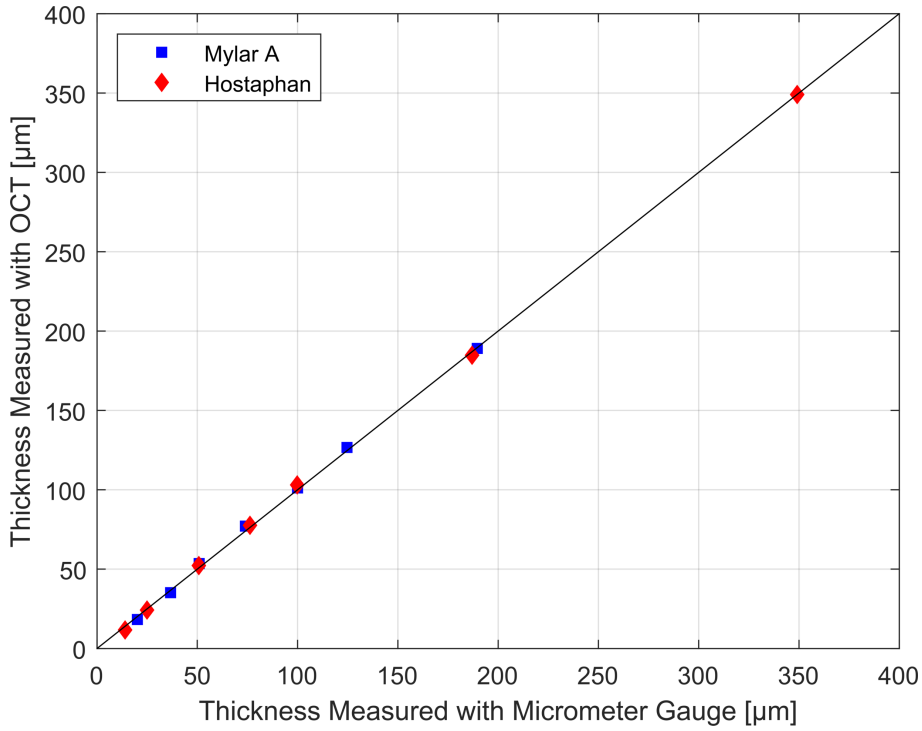

Figure 3: Comparison of 3-D OCT results for two PET-foils in relation to the reference method over a thickness range of 12 µm to 350 µm foil thickness. The graph is representative for 1D-OCT as well as for 3D-OCT measurements. For the sake of clarity only the 3-D data is shown.

3.3 Validating Coating Thickness of OCT Measurements performed on coated tablet samples

The results for the tablet coating layer thickness measurements for 3D-OCT and light microscopy measurements are summarized in Figure 4. The OCT and the light microscopy results for measurements acquired on the same tablet match very well, both for the Thrombo ASS and the Pantoloc samples.

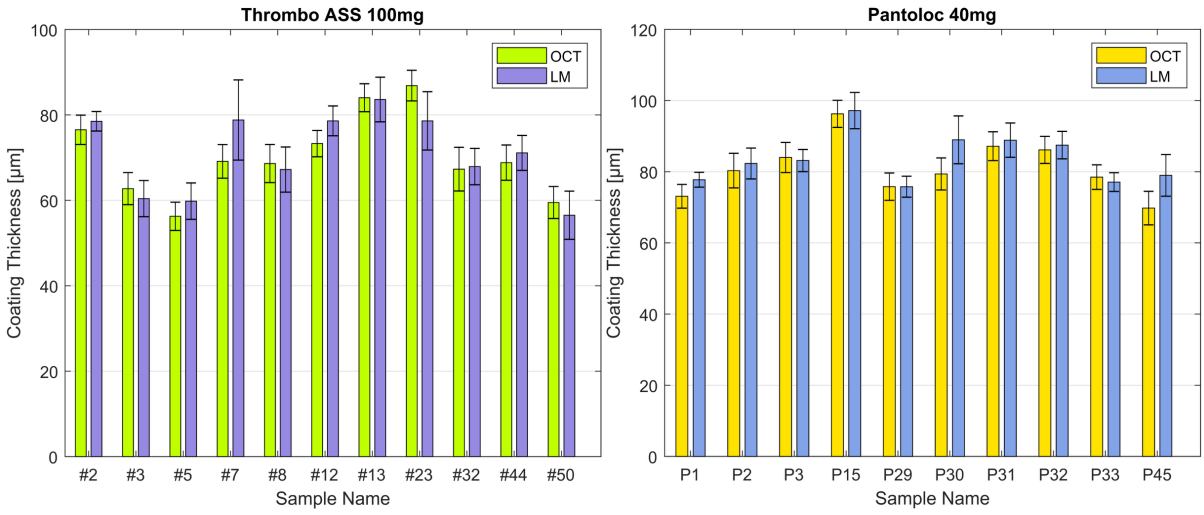

Figure 4: Results of average coating thickness and intra-coating variability measured via 3D-OCT and light microscopy measurements for individual Thrombo ASS and Pantoloc tablets

Although both techniques agree well with each other, the variation between tablets of the same type is unexpectedly high and is resolved both in OCT as well as the microscopy analysis of the cross-sectional images based on the microtome cuts. Coating thicknesses vary between 56.3 µm to 86.9 µm for the Thrombo ASS tablets and 69.8 µm to 97.2 µm for the Pantoloc tablets.

The results are summarized in Table 3, with additional information about the range of thickness variations in individual tablets (intra-tablet coating thickness variation). For the automated 1D-OCT measurements, these values are not deducible using the software applied in this study. The presented coating variability represent variations of the coating thickness on the tablet cap areas for all three approaches. Images of tablet edges or the tablet band during acquisition of the rotation drum measurements were intentionally automated rejected by the 1D system to ensure the same experimental input conditions for all experiments.

Table 3: Results for OCT and light microscopy measurements.

		3D-OCT (manual)	Light Microscopy	1D-OCT (automated)
Thrombo ASS 100mg	Mean [µm]	70.3	71.0	69.0
	SD (*inter*) [µm]	9.0	8.7	8.3
	SD (*intra*) [µm]	3.0 – 5.1	2.3 – 9.4	-
Pantoloc 40mg	Mean [µm]	81.0	83.7	81.0
	SD (*inter*) [µm]	7.3	6.5	7.3
	SD (*intra*) [µm]	3.3 – 4.9	2.1 – 6.7	-

4. DISCUSSION

4.1 PET Foils as a Validation Material – Comparison of Sensors

Reliable micrometer gauge measurements can only be carried out using free-standing, flat films. Pharmaceutical coatings are neither. They are firmly bonded to the tablet core and have high radii of

curvature in many locations on the tablet surface. Another drawback for the caliper method in the context of pharmaceutical film coatings is that it is time-consuming and operator-dependent. However, as a reference for the PET-films this method worked quite well and had an uncertainty of the measurements of 1.1 µm.

Among the three technologies suitable for non-destructive and calibration-free examination of tablet coatings tested, terahertz imaging offers the lowest spatial resolution due to the wavelength range applied. Moreover, the estimated resolution limit of about 35 µm agrees with the values in the literature (Zeitler and Gladden, 2009). Regardless of this limitation, the results of terahertz measurements are consistent with the reference and the other technologies tested. For film thicknesses above 36 µm for the transmission and above 50 µm for the reflectance measurements, the deviations from the reference are in the same order of magnitude as the competing technologies. In terms of pharmaceutical coatings, THz imaging has its advantages when it comes to monitoring the tablet coatings with scattering inorganic pigments and high layer thickness exceeding 150 µm. With regard to the PET films as a reference material, the THz results are plausible and indicate good linearity, even when considering the results below the resolution limit.

The X-ray microcomputer tomography (XµCT) measurements correlate well with the reference method, although the measured thickness tends to be slightly higher, as well as the SDs. This is surprising, as XµCT is considered a "gold standard" and a considerably long measurement time in combination with the technical effort suggests a higher accuracy of the results. Nevertheless, XµCT has the highest spatial resolution of the methods tested and offers full 3D volume information, including microstructural features that are not visible via OCT or THz. With regard to the PET films, the XµCT measurements agree well with the competing technologies, additionally showing that the various degrees of film thickness have the same microstructure. Tomograms of XµCT and 3D OCT measurements underline a high uniformity of the films in terms of thickness.

The OCT measurements agree very well with the reference and other methods. Particularly noteworthy are the constant low standard deviations for both 1D- and 3D-OCT measurements, which emphasize the high optical quality and homogeneity of the films and equipment used. The linearity of tested OCT systems was investigated for two different polyesters over wide thickness ranges of 19-190 µm for Mylar and 12-390 µm for Hostaphan, respectively, indicating excellent linearity and correlation with the reference method over the whole thickness range. The performance of our in-house prototype is comparable with the commercial OSeeT system, except for the convenience during operation and time effort for the measurements and evaluation of the commercial system.

The proposed approach of using PET foils as a validation target cannot replace the established reference targets, such as e.g. the Arden Photonics reference target for ultra-high resolution OCTs (UHR-OCTs) or for the measurement of point-spread-function and lateral resolution. However, it offers a very simple and reliable system for, even fully automated, performance verification and validation of industrial OCT systems.

4.2 Comparison of Reported Tablet Coating Thicknesses - Light Microscopy vs. OCT

The results for the light microscopy and OCT measurements correlate very well for both Thrombo ASS and Pantoloc tablets. The standard deviations are in the same range for both techniques except for the samples #7, #23 (Thrombo ASS) and P30 (Pantoloc). Comparing the results based on individual tablets, the performance of OCT and light microscopy (LM) is very consistent. However, the variation

between single tablets (inter-tablet coating thickness variation) is pronounced, with coating variabilities of 12.8% RSD (OCT) and 12.5% RSD (LM) for Thrombo ASS and 9.0% RSD (OCT) and 7.7% RSD (LM) for Pantoloc. Since the tablets tested are commercial tablets from a pharmacy and at least the Thrombo ASS tablets are all from one box and, according to the batch code on the blisters, from one batch, this high variation reflects the real variation in the existing coating processes. These findings are supported by the microscopy images in Figure 5, with a high variation of coating thickness along the intersection of the tablet. They are consistent with the literature for both in-line and off-line measurements of tablet coatings (Sacher et al., 2019; Wolfgang et al., 2019).

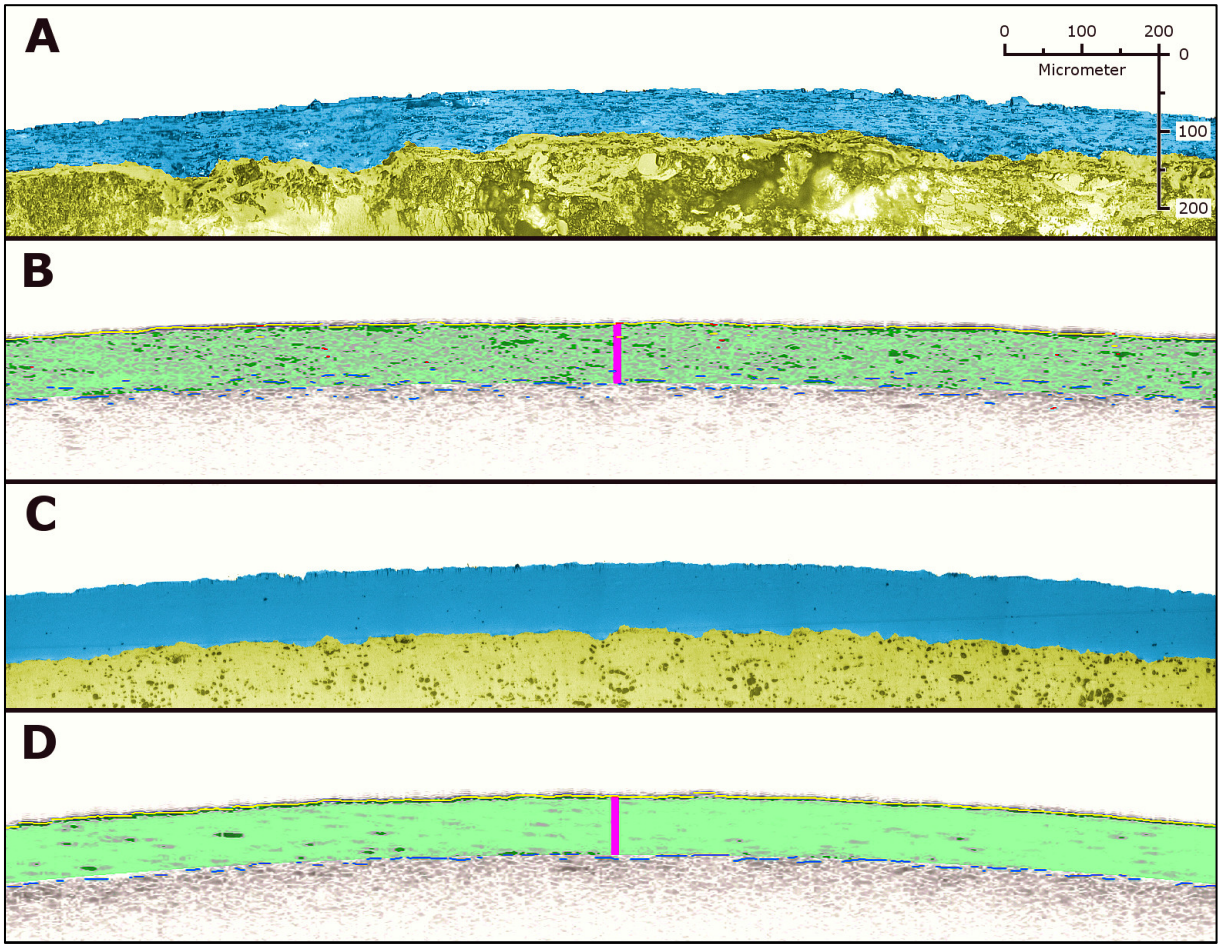

Figure 5: Detail of various Thrombo ASS (A, B) and Pantoloc tablets (C, D) recorded with light microscopy (A, C) and 3D-OCT (B, D). The intersection of A and C is presented by stitched microscopy images. Note a strong variation in the coating thickness, especially in A. For better visualization, the core is shaded yellow and the enteric coating blue for the light microscopy images. For the OCT images (B, D) the green band and the pink bar correspond to the features extracted via the automated evaluation algorithm. The scale is the same for all pictures.

As stated in the Material and Methods section and shown in Figure 5, no attempt to perfectly co-locate A, B and C, D were made, but the respective locations are very close to each other. The strong variation in Thrombo ASS picture (A) is not so obvious in the corresponding 3D-OCT image due to the overlay of the algorithmic features and strong scattering of the enteric coating containing a high amount of talc (approximately 30% talc in the dry coating according to technical notes on this coating system (Evonik Industries AG, 2014)).

The microscopy image evaluation was made manually by measuring the coating thickness in regular intervals over the entire cutting edge, as described in the materials and methods section. This resulted in a small number of measurements of 7-18 per sample, depending on the interface length available. In contrast, the automated evaluated 1D OCT measurements had a pre-set standardized measuring routine and only reported the tablet value when at least 50 measurements per interface or more were detected. Based on these data, a statistical evaluation of the readings can be performed. The 1D-OCT system evaluates the complete variation of a contiguous portion of the cross sections in the scanned area and calculates the coating thickness and its variation, as well the optical homogeneity of the layer and the surface roughness like presented by Markl et al. (Markl et al., 2018).

Comparing both techniques, the results demonstrate that OCT (1D and 3D) and light microscopy deliver consistent results. The OCT measurements seem to be more plausible in terms of a statistically sounder basis, especially for the automated 1D measurements, and can be performed destruction free, calibration free and within a few minutes. Our work demonstrates that automatically evaluated OCT measurements of commercial pharmaceutical coatings withstand a critical comparison with established technology for coating thickness evaluation.

5. SUMMARY AND CONCLUSIONS

This study demonstrates that biaxially stretched polyethylene terephthalate films can be applied ~~(even in an industrial environment)~~ to compare system performance of various sensor systems in terms of thickness measurements. Among the technologies tested, OCT appears to provide the most consistent results compared to the established reference methods. Due to the physical and chemical material properties and the applicability to all tested sensors, PET films can be considered an excellent model system for validating the measuring instruments for monitoring purposes in the pharmaceutical industry. Moreover, we believe that PET foils could serve in the future as a very economic and easy to use layer thickness standard for medical OCT applications too.

The comparison of measured coating thickness and its variation via 1D- and 3D-OCT as well as light microscopy on commercially-available tablets demonstrates the advantages and reliability of OCT. All results of 3D-OCT measurements and LM correlate very well. Fully automatic measurements and evaluation via 1D-OCT reports the same results as the reference method (LM) in a much shorter time. In addition, OCT measurements can provide further information about pharmaceutical coatings, such as surface roughness, defects and optical film homogeneity in real-time like presented in (Sacher et al., 2019).

Our results indicate that OCT can be used in the pharmaceutical industry for generating significant statistical data of mean coating thickness with information about inter- and intra-tablet coating thickness variability. Thus, OCT enables scientists and process engineers to achieve an enhanced understanding of the critical quality attributes of pharmaceutical coatings in real-time, including thickness, variability and coating quality, both intra- and inter-batch.

Acknowledgements

This work has been funded by the Austrian COMET Program under the auspices of the Austrian Federal Ministry of Transport, Innovation and Technology (bmvit), the Austrian Federal Ministry of Economy, Family and Youth (bmwfj) and by the State of Styria (Styrian Funding Agency SFG). COMET

is managed by the Austrian Research Promotion Agency FFG. Additionally, D. Markl and J. A. Zeitler would like to acknowledge the U.K. Engineering and Physical Sciences Research Council (EPSRC) for funding (EP/L019922/1).

REFERENCES

Amborski, L.E., Flierl, D.W., 1953. Physical Properties of Polyethylene Terephthalate Films. Ind. Eng. Chem. 45, 2290–2295. https://doi.org/10.1021/ie50526a042

Arden Photonics Ltd, 2018. APL-OP01 OCT phantom [WWW Document]. URL https://www.ardenphotonics.com/products/apl-op01/ (accessed 12.7.19).

Barimani, S., Kleinebudde, P., 2017. Evaluation of in–line Raman data for end-point determination of a coating process: Comparison of Science–Based Calibration, PLS-regression and univariate data analysis. Eur. J. Pharm. Biopharm. 119, 28–35. https://doi.org/10.1016/j.ejpb.2017.05.011

Bell, D.T., 2016. PET film artificial weathering: the action of degradation agents on bulk and surface properties.

Corcoran, A., Muyo, G., Van Hemert, J., Gorman, A., Harvey, A.R., 2015. Application of a wide-field phantom eye for optical coherence tomography and reflectance imaging. J. Mod. Opt. 62, 1828–1838. https://doi.org/10.1080/09500340.2015.1045309

de Boer, J.F., Leitgeb, R., Wojtkowski, M., 2017. Twenty-five years of optical coherence tomography: the paradigm shift in sensitivity and speed provided by Fourier domain OCT. Biomed. Opt. Express 8, 3248. https://doi.org/10.1364/BOE.8.003248

Dong, Y., Lin, H., Abolghasemi, V., Gan, L., Zeitler, J.A., Shen, Y.C., 2017. Investigating Intra-Tablet Coating Uniformity With Spectral-Domain Optical Coherence Tomography. J. Pharm. Sci. 106, 546–553. https://doi.org/10.1016/j.xphs.2016.09.021

DuPont Teijin Flms, 2003. Mylar - Product information [WWW Document]. URL http://usa.dupontteijinfilms.com/wp-content/uploads/2017/01/Mylar_Electrical_Properties.pdf (accessed 12.7.19).

Elman, J.F., Greener, J., Herzinger, C.M., Johs, B., 1998. Characterization of biaxially-stretched plastic films by generalized ellipsometry. Thin Solid Films 313–314, 814–818. https://doi.org/10.1016/S0040-6090(97)01001-8

Evonik Industries AG, 2014. Technical Information Eudragit® L 30 D-55 [WWW Document]. URL https://www.stobec.com/DATA/PRODUIT/1598~v~data_8595.pdf (accessed 12.7.19).

Gabriele Sandrian, M., Tomlins, P., Woolliams, P., Rasakanthan, J., Lee, G.C., Yang, A., Považay, B., Alex, A., Sugden, K., Drexler, W., 2012. Three-dimensional calibration targets for optical coherence tomography. Opt. Diagnostics Sens. XII Towar. Point-of-Care Diagnostics; Des. Perform. Valid. Phantoms Used Conjunction with Opt. Meas. Tissue IV 8229, 822914. https://doi.org/10.1117/12.907748

Ghim, Y.S., Rhee, H.G., Yang, H.S., Lee, Y.W., 2013. Thin-film thickness profile measurement using a Mirau-type low-coherence interferometer. Meas. Sci. Technol. 24. https://doi.org/10.1088/0957-0233/24/7/075002

Hu, Z., Hao, B., Liu, W., Hong, B., Li, J., 2014. Test target for characterizing 3D resolution of optical coherence tomography. Int. Symp. Optoelectron. Technol. Appl. 2014 Laser Opt. Meas. Technol. Fiber Opt. Sensors 9297, 92971S. https://doi.org/10.1117/12.2073062

Koller, D.M., Hannesschläger, G., Leitner, M., Khinast, J.G., 2011. Non-destructive analysis of tablet coatings with optical coherence tomography. Eur. J. Pharm. Sci. 44, 142–148. https://doi.org/10.1016/j.ejps.2011.06.017

Kühnhold, P., Nolvi, A., Tereschenko, S., Kassamakov, I., Hæggström, E., Lehmann, P., 2015. Transparent layer thickness measurement using low-coherence interference microscopy. Proc. SPIE - Int. Soc. Opt. Eng. 9525,

1–11. https://doi.org/10.1117/12.2184011

Li, C., Zeitler, J.A., Dong, Y., Shen, Y.C., 2014. Non-destructive evaluation of polymer coating structures on pharmaceutical pellets using full-field optical coherence tomography. J. Pharm. Sci. 103, 161–166. https://doi.org/10.1002/jps.23764

Lin, H., Dong, Y., Markl, D., Williams, B.M., Zheng, Y., Shen, Y., Zeitler, J.A., 2017. Measurement of the Intertablet Coating Uniformity of a Pharmaceutical Pan Coating Process With Combined Terahertz and Optical Coherence Tomography In-Line Sensing. J. Pharm. Sci. 106, 1075–1084. https://doi.org/10.1016/j.xphs.2016.12.012

Lin, H., Dong, Y., Shen, Y., Zeitler, J.A., 2015. Quantifying Pharmaceutical Film Coating with Optical Coherence Tomography and Terahertz Pulsed Imaging: An Evaluation. J. Pharm. Sci. 104, 3377–3385. https://doi.org/10.1002/jps.24535

Lin, H., Zhang, Z., Markl, D., Zeitler, J., Shen, Y., 2018. A Review of the Applications of OCT for Analysing Pharmaceutical Film Coatings. Appl. Sci. 8, 2700. https://doi.org/10.3390/app8122700

Manallah, A., Bouafia, M., Meguellati, S., 2015. Optical coherence tomography as film thickness measurement technique. Proc. SPIE - Int. Soc. Opt. Eng. 9450, 945006. https://doi.org/10.1117/12.2061387

Markl, D., Hannesschläger, G., Sacher, S., Leitner, M., Buchsbaum, A., Pescod, R., Baele, T., Khinast, J.G., 2015a. In-Line Monitoring of a Pharmaceutical Pan Coating Process by Optical Coherence Tomography. J. Pharm. Sci. 104, 2531–2540. https://doi.org/10.1002/jps.24531

Markl, D., Hannesschläger, G., Sacher, S., Leitner, M., Khinast, J.G., 2014. Optical coherence tomography as a novel tool for in-line monitoring of a pharmaceutical film-coating process. Eur. J. Pharm. Sci. 55, 58–67. https://doi.org/10.1016/j.ejps.2014.01.011

Markl, D., Wahl, P., Pichler, H., Sacher, S., Khinast, J.G., 2018. Characterization of the coating and tablet core roughness by means of 3D optical coherence tomography. Int. J. Pharm. 536, 459–466. https://doi.org/10.1016/j.ijpharm.2017.12.023

Markl, D., Zettl, M., Hannesschläger, G., Sacher, S., Leitner, M., Buchsbaum, A., Khinast, J.G., 2015b. Calibration-free in-line monitoring of pellet coating processes via optical coherence tomography. Chem. Eng. Sci. 125, 200–208. https://doi.org/10.1016/j.ces.2014.05.049

Mauritz, J.M.A., Morrisby, R.S., Hutton, R.S., Legge, C.H., Kaminski, C.F., 2010. Imaging Pharmaceutical Tablets with Optical Coherence Tomography. J. Pharm. Sci. 99, 385–391. https://doi.org/10.1002/jps.21844

Möltgen, C. V., Herdling, T., Reich, G., 2013. A novel multivariate approach using science-based calibration for direct coating thickness determination in real-time NIR process monitoring. Eur. J. Pharm. Biopharm. 85, 1056–1063. https://doi.org/10.1016/j.ejpb.2013.09.011

Müller, J., Knop, K., Thies, J., Uerpmann, C., Kleinebudde, P., 2010. Feasibility of Raman spectroscopy as PAT tool in active coating Raman spectroscopy as PAT tool in active coating. Drug Dev. Ind. Pharm. 36, 234–243. https://doi.org/10.3109/03639040903225109

Nemeth, A., Hannesschläger, G., Leiss-Holzinger, E., Wiesauer, K., Leitner, M., 2013. Optical Coherence Tomography – Applications in Non-Destructive Testing and Evaluation. Intech 163–185. https://doi.org/10.5772/53960

Sacher, S., Wahl, P., Weißensteiner, M., Wolfgang, M., Pokhilchuk, Y., Looser, B., Thies, J., Raffa, A., Khinast, J.G., 2019. Shedding Light on Coatings: Real-time Monitoring of Coating Quality at Industrial Scale. Int. J. Pharm. 566, 57–66. https://doi.org/10.1016/j.ijpharm.2019.05.048

Wahl, P.R., Peter, A., Wolfgang, M., Khinast, J.G., 2019. How to Measure Coating Thickness of Tablets: Method Comparison of Optical Coherence Tomography, Near-infrared Spectroscopy and Weight-, Height- and Diameter Gain. Eur. J. Pharm. Biopharm. https://doi.org/10.1016/j.ejpb.2019.06.021

Wolfgang, M., Wahl, P., Sacher, S., Gartshein, E., Khinast, J.G., 2019. Real-Time Measurement of Coating Film

522 Thickness. Pharm. Technol. 43, 36–47.

523 Yen, C.-T., Huang, J.-F., Wu, M.-J., Lee, Y.-F., Huang, C.-T., Huang, S.-F., Cheng, H.-C., 2014. Simultaneously
524 measuring the refractive index and thickness of an optical sample by using improved fiber-based optical
525 coherence tomography. Opt. Eng. 53, 044108. https://doi.org/10.1117/1.OE.53.4.044108

526 Yoshino, H., Abbas, A., Kaminski, P.M., Smith, R., Walls, J.M., Mansfield, D., 2017. Measurement of thin film
527 interfacial surface roughness by coherence scanning interferometry. J. Appl. Phys. 121.
528 https://doi.org/10.1063/1.4978066

529 Zeitler, J.A., Gladden, L.F., 2009. In-vitro tomography and non-destructive imaging at depth of pharmaceutical
530 solid dosage forms. Eur. J. Pharm. Biopharm. 71, 2–22. https://doi.org/10.1016/j.ejpb.2008.08.012

531 Zeitler, J.A., Shen, Y., Baker, C., Taday, P.F., Pepper, M., Rades, T., 2007. Analysis of coating structures and
532 interfaces in solid oral dosage forms by three dimensional terahertz pulsed imaging. J. Pharm. Sci. 96, 330–
533 340. https://doi.org/10.1002/jps.20789

534 Zhong, S., Shen, Y.C., Ho, L., May, R.K., Zeitler, J.A., Evans, M., Taday, P.F., Pepper, M., Rades, T., Gordon, K.C.,
535 Mller, R., Kleinebudde, P., 2011. Non-destructive quantification of pharmaceutical tablet coatings using
536 terahertz pulsed imaging and optical coherence tomography. Opt. Lasers Eng. 49, 361–365.
537 https://doi.org/10.1016/j.optlaseng.2010.11.003

538